Available online at www.sciencedirect.com
ScienceDirect
Journal of Computational Physics 227 (2008) 5072–5089
JOURNAL OF COMPUTATIONAL PHYSICS
www.elsevier.com/locate/jcp

Discrete thermal element modelling of heat conduction in particle systems: Basic formulations

Y.T. Feng *, K. Han, C.F. Li, D.R.J. Owen

Civil and Computational Engineering Centre, School of Engineering, Swansea University, Wales SA2 8PP, UK

Received 22 June 2007; received in revised form 17 December 2007; accepted 20 January 2008
Available online 2 February 2008

Abstract

This paper proposes a novel numerical methodology, termed the *discrete thermal element method* (DTEM), for the effective modelling of heat conduction in systems comprising a large number of circular particles in 2D cases. Based on an existing analytical integral solution for the temperature distribution over a circular domain subjected to the Neumann boundary condition, a linear algebraic system of thermal conductivity equations for each particle is derived in terms of the average temperatures and the resultant fluxes at the contact zones with its neighboring particles. Thus, each particle is treated as an individual element with the number of (temperature) unknowns equal to the number of particles that it is in contact with. The element thermal conductivity matrix can be very effectively evaluated and is entirely dependent on the characteristics of the contact zones, including the contact positions and contact angles. This new element shares the same form and properties with its conventional thermal finite element counterpart. In particular, the whole solution procedure can follow exactly the same steps as those involved in the finite element analysis. Unlike finite elements or other modern numerical techniques, however, no discretization errors are involved in the discrete thermal elements. The modelling error mainly stems from the assumption made about the heat flux distribution within the contact zones. Based on some theoretical work, an enhanced version is suggested to improve the approximation. The numerical assessment against finite element results indicates that the basic version of DTEM can achieve a very reasonable solution accuracy, while the enhanced version further improves the accuracy to a high level. In addition, thermal resistance phenomena between the contact zones can be readily incorporated into the current modelling framework.

Keywords: Discrete thermal element method; Circular particle; Thermal contact; Heat conduction; Boundary (integral) equation/element

1. Introduction

Heat transfer in particle systems can be encountered in many engineering and scientific applications, for instance, in porous media, soil and geo-mechanics, civil, chemical and nuclear engineering, and materials processing. Although effective numerical thermal analysis techniques, predominantly finite element method based

* Corresponding author. Tel.: +44 1792 295161; fax: +44 1792 295676.
E-mail address: y.feng@swansea.ac.uk (Y.T. Feng).

0021-9991/$ - see front matter © 2008 Elsevier Inc. All rights reserved.
doi:10.1016/j.jcp.2008.01.031

(FEM) [1], have been well established for various types of problems, the modelling of heat transfer in systems comprising a large number of particles remains a computational challenge, particularly when coupled with other physical phases such as solid and fluid media.

In general, two different approaches have been proposed to undertake thermal analysis of problems involving particles. When a particle system can be treated as a porous medium, a 'smeared' continuous approach is often adopted where the effective macroscopic properties (assumed homogenous) of the system is generally determined by a detailed thermal analysis using the finite element method (FEM), for instance, by taking a small scale micro-structure of the system or a representative volume element. The most attractive feature of such an approach is that it can utilize the established continuum based methods to achieve a high computational efficiency for large scale problems. Nevertheless the approach cannot easily account for structural variations at both spatial and particle levels. There are a number of emerging applications where the consideration of features at all scales may be essential. Theoretically, any type of heat transfer problem can be modelled by FEM. However, FE methods would be extremely inefficient to model the entire particle system due to an excessively large scale finite element model resulting from the discretizition of each particle. In this context, the boundary element method [2,3] seems to be a better option since only the boundary of a particle needs to be discretized, which gives rise to a much smaller numerical system in comparison with the FEM, though this possibility has not been fully exploited, to our best knowledge. Clearly more efficient thermal modelling technologies are required for large scale particle systems.

On the other hand, some attempts have been made in which the particles are individually represented but by a much simplified model. One notable approach, termed the thermal network [4], represents each particle as an isothermal disk/sphere and each pair of contacting particles by an equivalent thermal resistance *bar* or *pipe* so that the thermal equations of the whole system can be modelled in terms of the corresponding thermal resistance/conduction network. Although simple and computationally efficient, the isothermal assumption made in the model over simplifies the actual thermal behavior of particles and limits its applicability for transient cases [4]. In a different approach proposed in [5], the particle system is represented as a Voronoi polyhedron, and the effective conductivity of the packing is modelled again by network-type analyzes. The common feature of the above two approaches is that the determination of the thermal properties/parameters in the models is based more on an ad hoc manner than on a rigorous theoretical foundation, which may introduce modelling errors that are difficult to quantify and control.

Furthermore, heat transfer within a particulate system is often closely coupled with particle mechanical contact and/or fluid flows. Over the last decade or so, many coupled numerical techniques have been developed to account for the interactions between different physical phases. Some latest developments have focused on the accurate modelling of different phases and their coupling in particle transport problems (see for instance [6]). Coupling of discrete elements with Navier–Stokes equations for particle–fluid interaction problems has been extensively used for the modelling of fluidized beds [7,8]. A simple particle–particle heat transfer model, analogous to the standard discrete elements for solids, has also been introduced [9] to account for thermal effects. This particle thermal model is nevertheless similar to the thermal network approach mentioned earlier and thus suffers from poor accuracy. In the coupled Lattice Boltzmann method (LBM) [10] and the discrete element method (DEM) [11] for particle–fluid interaction problems [12–15], (turbulent) fluid flows are modelled by the LBM while individual solid particles are described by the DEM, and the particle–fluid interaction can be accurately calculated through a suitable boundary condition. Although extension to include heat conduction has also been achieved, currently available thermal Lattice Boltzmann formulations [16,17] are not efficient for simulating heat conduction in systems comprising a large number of particles.

The main objective of this paper is therefore to propose a novel numerical methodology for accurate and effective modelling of heat conduction in individual particles as well as particulate systems in 2D cases. Under the assumptions that particles are circular disks and conduction is the dominant heat transfer mechanism in the problem, the proposed approach, termed the *discrete thermal element method* (DTEM), provides a very simple but accurate description of heat conduction within the system. Consequently, the approach can be employed to replace or improve the accuracy/efficiency of existing particle thermal models and to very effectively simulate heat conduction in systems comprising a large number of particles.

The development of the DTEM is motivated conceptually by the boundary element method (BEM) where only the boundary of a particle needs to be discretized. Its final form closely resembles finite element

formulations. Specifically, by utilizing an existing analytical integral solution for the temperature distribution over a circular domain subjected to the Neumann boundary condition (not included in [18]), a much simpler linear thermal conductivity equation is established for the particle, between the average temperatures and resultant fluxes at the contact zones of a particle with its adjacent particles. Thus, the only unknown variables for each particle are the average temperatures at the contact zones, which typically number around 3 or 4.

The paper is organized as follows: in Section 2, the integral solution to heat conduction in a circular domain is introduced. Then the details of the proposed DTEM are described in Section 3. Additional issues associated with the DTEM are discussed in Section 4. Two examples are provided in Section 5 to assess the solution accuracy of the method against FEM and to demonstrate its effectiveness. The main features of the proposed methodology are summarized in Section 6.

2. Analytical solution of temperature distribution in a circular domain

Consider a 2D circular domain of radius R with an isotropic thermal conductivity κ and subjected to a prescribed heat flux (Neumann) boundary condition as shown in Fig. 1. Using a polar coordinate system with the origin set at the centre of the domain $\Omega = \{(r,\theta) : 0 \leqslant r \leqslant R;\ 0 \leqslant \theta \leqslant 2\pi\}$, the temperature distribution in the domain is governed by the Laplace equation as

$$\begin{cases} \kappa \Delta T = 0 & \text{in } \Omega \\ \kappa \frac{\partial T}{\partial n} = q(\theta) & \text{on } \partial\Omega \end{cases} \tag{1}$$

where $\partial\Omega$ denotes the boundary (circumference) of the domain, and n is the outward normal to the boundary. Note that the flux $q(\theta)$ inward to the boundary is assumed positive. The temperature at any point $(r,\theta) \in \Omega$ can be expressed by the so-called Dini's integral [19] as

$$T(r,\theta) = -\frac{R}{2\pi\kappa}\int_0^{2\pi} q(\phi)\ln\left[1 - 2\frac{r}{R}\cos(\theta-\phi) + \left(\frac{r}{R}\right)^2\right]\mathrm{d}\phi + C \tag{2}$$

where C is a constant. The existence of this solution requires

$$\int_0^{2\pi} q(\theta)\mathrm{d}\theta = 0 \tag{3}$$

which is physically equivalent to the global heat flux equilibrium of the domain. It is easy to verify that the temperature at the centre $T_o = T(0,0) = C$. Thus,

$$T(r,\theta) = -\frac{R}{2\pi\kappa}\int_0^{2\pi} q(\phi)\ln\left[1 - 2\frac{r}{R}\cos(\theta-\phi) + \left(\frac{r}{R}\right)^2\right]\mathrm{d}\phi + T_o \quad (r,\theta) \in \Omega \tag{4}$$

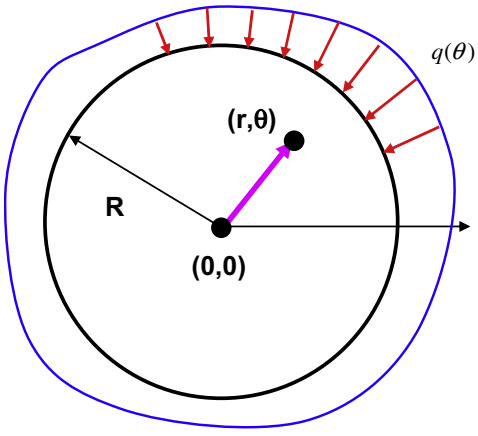

Fig. 1. Circular domain with Neumann boundary condition.

Then the temperature on the boundary is obtained as

$$T_c(\theta) = T(R,\theta) = -\frac{R}{2\pi\kappa}\int_0^{2\pi} q(\phi)\ln[2-2\cos(\theta-\phi)]\mathrm{d}\phi + T_o \quad (0 \leqslant \theta \leqslant 2\pi) \tag{5}$$

By utilizing the condition (3), the above formula can be rewritten as

$$T_c(\theta) = -\frac{R}{\pi\kappa}\int_0^{2\pi} q(\phi)\ln\left|\sin\frac{\theta-\phi}{2}\right|\mathrm{d}\phi + T_o \tag{6}$$

The significance of this solution is its *explicit evaluation* nature. Recall that only a Fredholm integral equation of the second type arises in the BEM [2,3], which then has to be solved numerically. Note that solution (6) is the basis for the development of the discrete thermal element approach described below.

According to the mean value theorem for Laplace's equation [19], the maximum and minimum values of the temperature are always achieved on the boundary $\partial\Omega$. In addition, the temperature at the centre of the domain, T_o, is the average value along any circle centered at the origin within the domain:

$$T_o = \frac{1}{2\pi}\int_0^{2\pi} T(r,\theta)\mathrm{d}\theta \quad (0 < r \leqslant R) \tag{7}$$

Particularly,

$$T_o = \frac{1}{2\pi}\int_0^{2\pi} T_c(\theta)\mathrm{d}\theta \tag{8}$$

It can be deduced that T_o is also the average temperature over the whole domain:

$$T_o = \frac{1}{\pi R^2}\int_\Omega T(r,\theta)\mathrm{d}\Omega \tag{9}$$

3. Discrete thermal element method

Consider a particle assembly subjected to a thermal boundary condition, as shown in Fig. 2a, in which each particle may be in contact with a number of adjacent particles, and heat is conducted through the contact zones between the particles. Note that it can be considered that the particles are brought into contact not only under mechanical forces but also being 'cemented' or bonded, as illustrated in Fig. 2b.

Let us isolate an arbitrary particle that is in contact with n neighboring particles. (Unknown) heat flux distributions are imposed over the n isolated contact zones on the boundary of the particle, and the remainder of

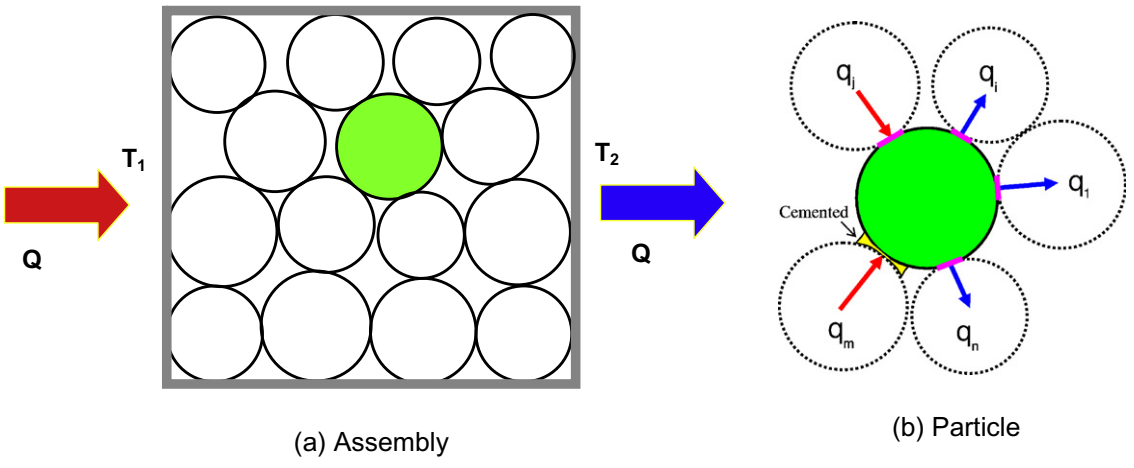

Fig. 2. Heat conduction in a simple particle system.

the particle boundary is assumed fully insulated, as shown in Fig. 3. Here the contact zones are assumed as circular arcs, although they may be flat or other shapes under mechanical contact [20]. This approximation may be acceptable as contact normally occurs over a small region. In addition, each contact zone is described by both the position, in terms of the angle θ of its middle point, and the (half) contact angle α that determines the contact arc length. Generally, the position angles θ_i are well spaced along the boundary and the contact angles α_i are small. For a dense packing, the average coordination number of particles, i.e. the value of n, is around 3–4. The positions and contact angles, θ_i and α_i, of all the n contact zones constitute the local element (thermal contact) configuration of the particle. Note that the particle radius R plays no direct role in the formulation, as will be shown later.

Next the heat conduction over the entire particle is to be represented with a *discrete* relation between the average temperatures and resultant fluxes at the n contact zones.

3.1. Discrete temperature distribution on particle boundary

The boundary flux condition in (1) can be refined for the special case shown in Fig. 3 as follows:

$$q(\theta) = \begin{cases} q_i(\theta - \theta_i) & \theta_i - \alpha_i \leqslant \theta \leqslant \theta_i + \alpha_i \ (i = 1, \ldots, n) \\ 0 & \text{otherwise} \end{cases} \tag{10}$$

From (6), the temperature on the boundary becomes

$$T_c(\theta) = -\frac{R}{\pi\kappa} \sum_{j=1}^{n} \int_{\theta_j - \alpha_j}^{\theta_j + \alpha_j} q(\phi) \ln \left| \sin \frac{\theta - \phi}{2} \right| \mathrm{d}\phi + T_o \tag{11}$$

or

$$T_c(\theta) = -\frac{R}{\pi\kappa} \sum_{j=1}^{n} \int_{-\alpha_j}^{\alpha_j} q_j(\phi) \ln \left| \sin \frac{\theta - \phi - \theta_j}{2} \right| \mathrm{d}\phi + T_o \tag{12}$$

and the temperature distribution along the ith contact arc is

$$T_c^i(\theta) = -\frac{R}{\pi\kappa} \sum_{j=1}^{n} \int_{-\alpha_j}^{\alpha_j} q_j(\phi) \ln \left| \sin \frac{\theta - \phi - \theta_j}{2} \right| \mathrm{d}\phi + T_o \quad (\theta_i - \alpha_i \leqslant \theta \leqslant \theta_i + \alpha_i) \tag{13}$$

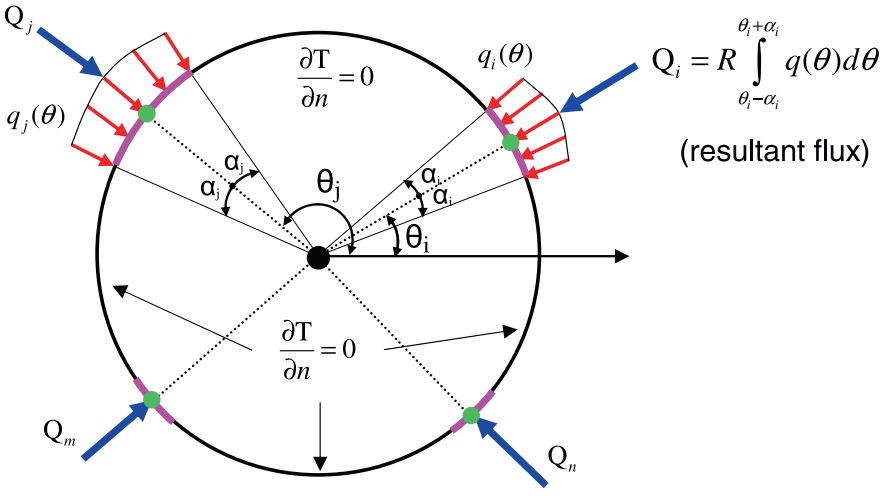

Fig. 3. Problem description of heat conduction in a circular particle.

By defining the resultant flux Q_i and the average temperature T_i on the ith arc, respectively, as

$$Q_i = R\int_{-\alpha_i}^{\alpha_i} q_i(\theta)\mathrm{d}\theta \tag{14}$$

$$T_i = \frac{1}{2\alpha_i}\int_{\theta_i-\alpha_i}^{\theta_i+\alpha_i} T_{\mathrm{c}}^{i}(\theta)\mathrm{d}\theta \tag{15}$$

and assuming that $q_i(\theta)$ is *constant* over the ith arc, i.e. $q_i(\theta) = \bar{q}_i$, the resultant Q_i becomes

$$Q_i = 2\alpha_i R\bar{q}_i \tag{16}$$

According to Eqs. (13) and (16), the average temperature T_i over the arc can be obtained as

$$T_i = \frac{1}{2\alpha_i}\int_{\theta_i-\alpha_i}^{\theta_i+\alpha_i}\left[-\frac{R}{\pi\kappa}\sum_{j=1}^{n}\int_{-\alpha_j}^{\alpha_j}\bar{q}_j\ln\left|\sin\frac{\theta-\phi-\theta_j}{2}\right|\mathrm{d}\phi\right]\mathrm{d}\theta + T_{\mathrm{o}} \tag{17}$$

or

$$T_i = \sum_{j=1}^{n}\left[-\frac{Q_j}{4\pi\kappa\alpha_i\alpha_j}\int_{-\alpha_i}^{\alpha_i}\int_{-\alpha_j}^{\alpha_j}\ln\left|\sin\frac{\Delta\theta_{ij}+\theta-\phi}{2}\right|\mathrm{d}\phi\,\mathrm{d}\theta\right] + T_{\mathrm{o}} \tag{18}$$

where $\Delta\theta_{ij} = \theta_i - \theta_j$, which is the angle 'distance' between the ith and jth arcs. The above equation can be expressed compactly as

$$T_i = \sum_{j=1}^{n} h_{ij}Q_j + T_{\mathrm{o}} \quad (i = 1,\ldots,n) \tag{19}$$

where

$$h_{ij} = -\frac{1}{4\pi\kappa\alpha_i\alpha_j}\int_{-\alpha_i}^{\alpha_i}\int_{-\alpha_j}^{\alpha_j}\ln\left|\sin\frac{\Delta\theta_{ij}+\theta-\phi}{2}\right|\mathrm{d}\phi\,\mathrm{d}\theta \tag{20}$$

Eq. (19) essentially establishes an *explicit*, *linear algebraic* system of equations for the average temperature on a contact arc and all the (resultant) fluxes acting on the contact zones, which provides the theoretical foundation for the development of the discrete thermal element.

The double integrals in formula (20) are inter-changeable and the integrand is always negative, therefore

$$h_{ij} = h_{ji} > 0 \tag{21}$$

Also note that the heat flux equilibrium condition (3) changes to

$$\sum_{i=1}^{n} Q_i = 0 \tag{22}$$

3.2. Discrete thermal element equations

By introducing the element temperature and flux vectors,

$$\mathbf{T}_{\mathrm{e}} = \{T_1,\ldots,T_n\}^{\mathrm{T}} \quad \text{and} \quad \mathbf{Q}_{\mathrm{e}} = \{Q_1,\ldots,Q_n\}^{\mathrm{T}}$$

and the element *thermal resistance* matrix $\mathbf{H}_{\mathrm{e}}$,

$$\mathbf{H}_{\mathrm{e}} = [h_{ij}]_{n\times n} \tag{23}$$

as well as a $n\times 1$ vector with all components of unity, $\mathbf{e} = \{1,\ldots,1\}^{\mathrm{T}}$, Eq. (19) can be expressed in matrix form as

$$\mathbf{T}_{\mathrm{e}} - \mathbf{e}T_{\mathrm{o}} = \mathbf{H}_{\mathrm{e}}\mathbf{Q}_{\mathrm{e}} \tag{24}$$

This is the element heat conduction equation in terms of thermal resistance. The equation possesses the following features: (1) the resistance matrix $\mathbf{H}_e$ is *symmetric* (cf. Eq. (21)); (2) the temperatures $\mathbf{T}_e$ are decoupled and thus no simultaneous equations need to be solved for determining the temperature when the fluxes $\mathbf{Q}_e$ are known. These two properties are a distinct advantage over the conventional boundary element formulation in which the corresponding matrix $\mathbf{H}$ is generally unsymmetric and the nodal temperatures are coupled.

Though not mathematically proved, $\mathbf{H}_e$ is invertible. Let

$$\widehat{\mathbf{K}}_e = \mathbf{H}_e^{-1} \tag{25}$$

then the inverse form of Eq. (24) reads

$$\widehat{\mathbf{K}}_e(\mathbf{T}_e - \mathbf{e}T_o) = \mathbf{Q}_e \tag{26}$$

Note that in both (24) and (26), the discrete temperatures $\mathbf{T}_e$ are relative values to the average temperature T_o which is as yet unknown. Thus, a further treatment is required so that equations (24) and (26) are fully solvable.

The total heat balance condition (3) can be rewritten as

$$\mathbf{e}^T\mathbf{Q}_e = 0 \tag{27}$$

Multiplying (26) by $\mathbf{e}^T$ gives

$$T_o = \mathbf{g}_e^T\mathbf{T}_e/\kappa_e \quad (\mathbf{g}_e = \widehat{\mathbf{K}}_e\mathbf{e},\ \kappa_e = \mathbf{e}^T\mathbf{g}_e) \tag{28}$$

i.e. the average temperature of the particle can be readily obtained by a linear combination of the discrete boundary temperature $\mathbf{T}_e$. This new formula can thus be viewed as the discrete version of the mean value condition (28). In addition, κ_e may be interpreted as the total element conductivity.

Based on relation (28), eliminating T_o from Eq. (26) leads to the following equation

$$\mathbf{K}_e\mathbf{T}_e = \mathbf{Q}_e \tag{29}$$

where

$$\mathbf{K}_e = \widehat{\mathbf{K}}_e - \mathbf{g}_e\mathbf{g}_e^T/\kappa_e \tag{30}$$

is the so-called element conductivity matrix.

Eq. (29) is essentially the heat conduction equation in discrete form for the particle, which formally defines the *discrete thermal element*, and all the associated formulations are described by (19), (20) and (28).

A very important feature of (29), and thus this new thermal element, is that it has an identical form as a finite element thermal element. In addition, it is easy to verify that

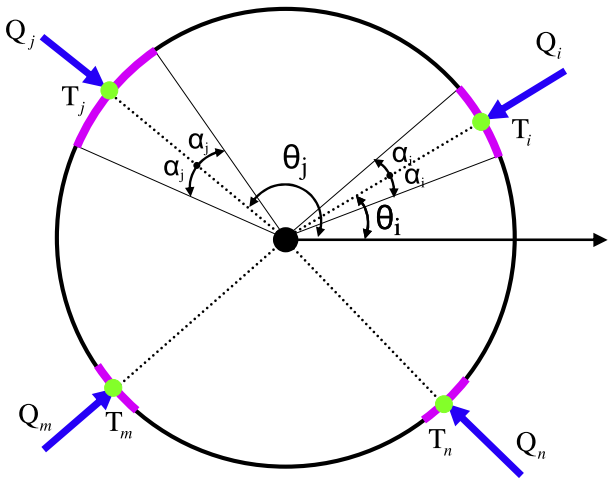

Fig. 4. Discrete thermal element.

$$\mathbf{K}_e = \mathbf{K}_e^T, \quad \mathbf{K}_e\mathbf{e} = \mathbf{0} \tag{31}$$

i.e. $\mathbf{K}_e$ is symmetric and singular, as in the case of finite element formulations. Clearly only temperatures are the primary variables, while the local fluxes will be eliminated in the subsequent global assembly stage. These features are different from the standard boundary elements where both nodal temperatures and fluxes are the system variables and the resulting matrices are unsymmetric in nature.

Fig. 4 depicts a general discrete thermal element, where the number of nodes n equals the number of neighboring particles in contact and thus can vary from element to element; each contact zone i is represented by a node and the list of all the contact zones *in any order* serves as the element connectivity; while the contact positions θ_i and angles α_i are the geometric properties of the element.

In other words, each circular particle can be viewed as a special shaped finite thermal element, although both approaches stem from different principles. The immediate consequence is that the subsequent procedure in this discrete thermal element method to model the assembled particle system can follow the same steps as used in FEM.

3.3. Thermal resistance matrix $\mathbf{H}_e$

The main computational issue associated with the formulation of the discrete thermal element proposed above is the evaluation of the coefficients of the resistance matrix, h_{ij}. Two distinct cases need to be considered:

Case 1: $i = j$. In this case, the formula for h_{ii} is

$$h_{ii} = -\frac{1}{4\pi\kappa\alpha_i^2}\int_{-\alpha_i}^{\alpha_i}\int_{-\alpha_i}^{\alpha_i} \ln\left|\sin\frac{\theta-\phi}{2}\right| \mathrm{d}\phi\,\mathrm{d}\theta \tag{32}$$

Clearly, h_{ii} is solely determined by the contact angle α_i. As the integrand $\ln|\sin(\theta-\phi)/2|$ is singular at $\phi = \theta$, some caution must be taken when numerically evaluating the above double integral. It can however be simplified into a single integral as follows:

$$h_{ii} = -\frac{2}{\pi\kappa}\int_0^1 (1-x)\ln[\sin(\alpha_i x)]\mathrm{d}x \tag{33}$$

Then the singularity appears only at $x = 0$. This integral may be effectively solved by employing, for instance, a special Gaussian rule for singular functions (see [21] for more detail). Further effort has led to an explicit approximation formula for h_{ii} with very high accuracy as follows:

$$h_{ii} = \frac{1}{\pi\kappa}\left(-\ln\alpha_i + \frac{3}{2} + \frac{\alpha_i^2}{36} + \frac{\alpha_i^4}{2700} + \frac{\alpha_i^6}{79,380} + \frac{\alpha_i^8}{252,000}\right) \tag{34}$$

Fig. 5a shows the value of h_{ii} as a function of the contact angle $\alpha_i \in (0, \pi/2]$ (assuming $\kappa = 1$), where h_{ii} is monotonically reduced from infinite at $\alpha_i = 0$ to the minimum value of 0.356322 at $\alpha_i = \pi/2$. The higher order terms of α_i in (34) may not be necessary for small contact angles. Fig. 5b depicts the accuracy of the above formula (34) for different contact angles, along with the accuracy of using only up to the terms α_i^4 and α_i^2. Clearly using only the first three terms (up to α_i^2) are normally sufficient for contact angles smaller than 30°.

Case 2: $i \neq j$. In this case, the integrand $\ln|\sin(\Delta\theta_{ij} + \theta - \phi)/2|$ is well-behaved and the normal 2×2 Gaussian quadrature over a rectangular domain $[-\alpha_i, \alpha_i] \times [-\alpha_j, \alpha_j]$ can be used to compute h_{ij} to a high level of accuracy. For small contact angles α_i and α_j, using only one Gaussian point at $(0,0)$, the centre of the integration domain, may be sufficient. Thus, h_{ij} can be evaluated by the following first order approximation:

$$h_{ij} = -\frac{1}{\pi\kappa}\ln|\sin(\theta_i - \theta_j)/2| \tag{35}$$

i.e. h_{ij} is mainly determined by the angle difference between the two contact zones. Given that the two contact zones involved have the same contact angle, the dependence of h_{ij} (relative to h_{ii}) on the angle

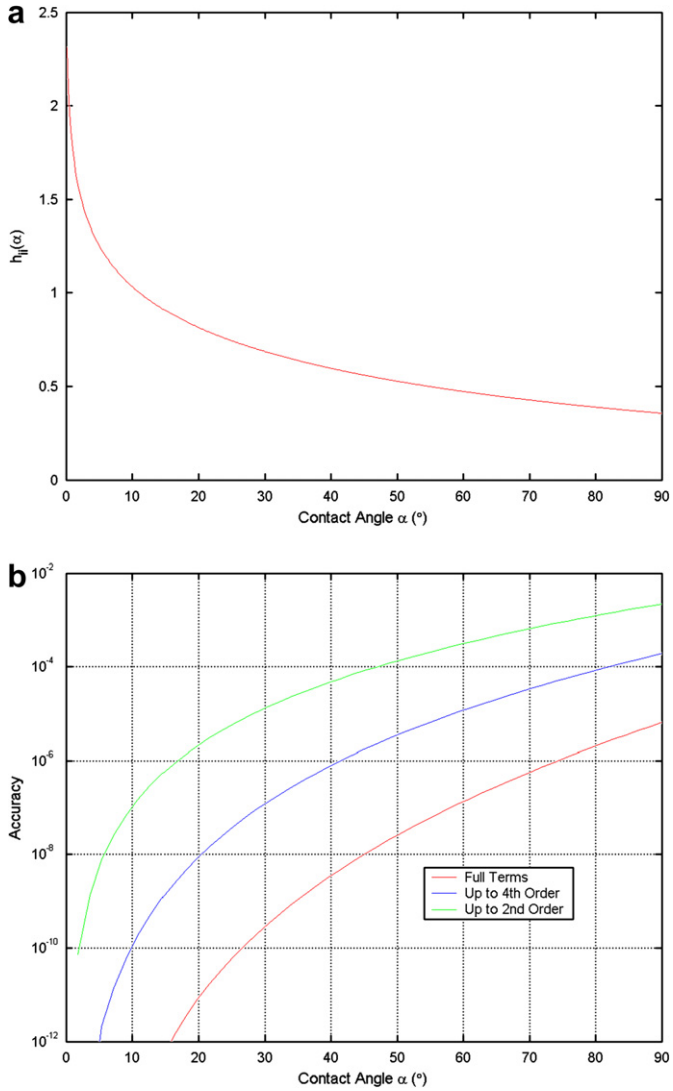

Fig. 5. (a) Value of h_{ii} vs. contact angle; (b) accuracy of the approximation formula (34).

difference $|\theta_i - \theta_j|$ is illustrated in Fig. 6 for three different contact angles $\alpha = 2.5°$, 5° and 10°. Smaller angle difference, i.e. closer contact zones, corresponds to a larger h_{ij}, implying a stronger coupling between the two zones; whereas a larger angle difference results in a weaker coupling effect. When the two zones are separated by 180°, h_{ij} is almost zero. h_{ij} is generally about one order smaller than h_{ii} for a reasonably small contact angle as the angle difference between any two contact zones is normally larger than 60°.

Remark: Formulae (34) and (35) not only demonstrate that the thermal resistance matrix of the element can be highly effectively evaluated, but also identify some intrinsic characteristics of heat conduction in a circular particle – the thermal resistance properties of a particle can be solely determined by its thermal contact geometric configuration, in which the contact angles α_i play a major role, and the contact positions θ_i play a minor role, while the size of the particle has no direct effect.

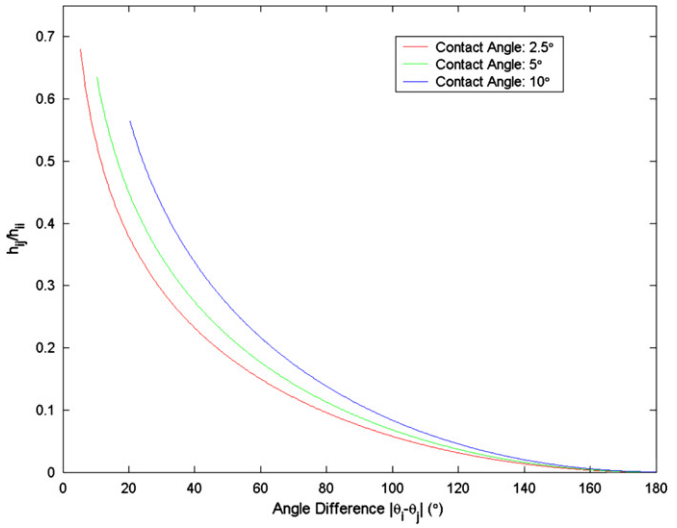

Fig. 6. Values of h_{ij}/h_{ii} vs. angle differences.

These features may not be readily apparent, as existing models often take particle size and distance between two contacting particles as the main parameters to determine the thermal resistance/conductivity of a particle. It is true that for two discrete particles brought together under mechanical forces, the corresponding configuration of the contact zone is closely related to the geometrical properties of the particles, i.e. the contact angle α is a function of the particle sizes and their distance. However, for particles that are 'cemented' or bonded together, the distance between the particles is irrelevant to the contact configuration. Therefore, the use of both contact angles and positions in this approach is a simple and universal representation of the thermal contact geometrical features of a particle.

3.4. The solution procedure of the discrete thermal element method

The discrete thermal element method shares the same form as the finite element formulation, and can follow the same computational steps used in the conventional finite element procedure to solve the heat conduction problem in a particle system. The main steps include: (1) preprocessing to obtain all element configurations and the relevant global information; (2) evaluating element conductivity matrices; (3) assembling the element contributions to form a global linear system of equations; (4) imposing boundary conditions; (5) solving the equations to find the discrete temperature values; and (6) postprocessing, if necessary, to compute the average temperature for each particle as well as the temperature at any point.

Based on the positions and radii of particles, the contact links (zones) between the particles can be established by employing any search algorithm commonly used in DEM (see, for instance [22]). Each link is equivalent to a node in a finite element model and is thus assigned a global nodal number. The total number of unknowns in the global system is equal to the number of contact links, which is about two times the number of particles. The list of the contact links associated with a particle serves as its element connectivity, and the contact positions and angles are the associated element geometric properties.

Assuming an average temperature at the contact zone and a zero net flux, i.e. no external heat source applied, the following global heat conduction equations can be established by assembling the contributions from all the particles:

$$\mathbf{KT} = \mathbf{Q} \tag{36}$$

where $\mathbf{K}$ is the global conductivity matrix; $\mathbf{T}$ is the global temperature vector including all the average temperature values at the contact regions; and $\mathbf{Q}$ is the global flux (load) vector with the majority of the components being zero if internal heat sources are not considered. The total number of global unknowns equals the total number of contact pairs in the particle system. Note that $\mathbf{K}$ is symmetric and sparse.

With appropriate boundary conditions imposed, the resulting global system of equations (36) can be solved by employing one of the advanced sparse matrix solution algorithms. In particular, when the current method is coupled with DEM, an explicit (pseudo-)time integration scheme, similar to the central difference algorithm, can also be adopted. It has been established that under certain conditions the central difference time integration is equivalent to the conjugate gradient method [23]. Clearly, systems with many thousands of particles can be effectively modelled.

After the temperatures at the contact zones are obtained, the average temperature of each particle, T_o, can be readily calculated according to formula (28). The element flux vector $\mathbf{Q}_e$ can be computed from Eq. (24). The temperature at any position within the particle domain can also be obtained as follows:

$$T(r,\theta) = -\frac{1}{2\pi\kappa}\sum_{i=1}^{n}\frac{Q_i}{2\alpha_i}\int_{-\alpha_i}^{\alpha_i}\ln\left[1-2\frac{r}{R}\cos(\theta-\theta_i-\phi)+\left(\frac{r}{R}\right)^2\right]\mathrm{d}\phi + T_o \tag{37}$$

The whole solution procedure of the proposed discrete thermal element method for modelling heat condition in a particle system is summarized in Box 1.

Box 1: Discrete thermal element method

1. Pre-processing
   - Given a particle assembly, establish the contact links between the particles.
   - For each particle, identify all the associated contact links/zones and determine the corresponding contact positions (θ_i) and the contact angles (α_i).
2. Element thermal conductivity computations. Loop over all particles,
   - Evaluate h_{ii} and h_{ij} from (34) and (20) to form $\mathbf{H}_e$.
   - Compute $\widehat{\mathbf{K}}_e = \mathbf{H}_e^{-1}$.
   - Determine the element conductivity matrix $\mathbf{K}_e$ based on (30).
3. Assemble. Based on the global contact links, assemble the element matrices $\mathbf{K}_e$ to form the matrix $\mathbf{K}$.
4. Impose boundary conditions to (36).
5. Solve the global system of equations (36) to obtain the temperatures at the contact zones.
6. Post-processing, if necessary.

4. Additional issues

4.1. Approximation errors

Unlike finite or boundary elements, there is no domain discretization involved in the current discrete thermal elements, thus no discretization error will occur. Modelling errors however stems from two sources.

Apart from the slightly inaccurate geometry description for the contact zones, the most significant assumption made in the development of the discrete thermal element formulations is that the flux distribution is constant over the contact arc, which is not the case in reality. In order to fully understand the thermal behavior within the contact zone, a theoretical analysis is conducted.

Consider two contacting disks with radii R_A and R_B and the corresponding contact angles α_A and α_B, respectively, as shown in Fig. 7a. A pair of point heat sources, Q and $-Q$ are applied to Points E and F at the far ends of the two disks, respectively. The flux distribution along the arc CHD is found to be

$$q(\phi) = -\frac{Q}{2\alpha_A R_A}w(\phi), \quad \phi \in (-\alpha_A, \alpha_A) \tag{38}$$

where

$$w(\phi) = \frac{2\alpha_A\beta\sin(\alpha_A)\sin(\pi\beta)}{\pi\beta}\frac{f_1^{2\beta}+f_2^{2\beta}}{\left[f_1^{4\beta}+f_2^{4\beta}-2f_1^{2\beta}f_2^{2\beta}\cos(2\pi\beta)\right](f_1 f_2)^{1-\beta}} \tag{39}$$

with $\beta = \pi/\gamma,\ \gamma = 2\pi - \alpha_A - \alpha_B,\ f_1 = \sin[(\alpha_A+\phi)/2],\ f_2 = \sin[(\alpha_A-\phi)/2]$.

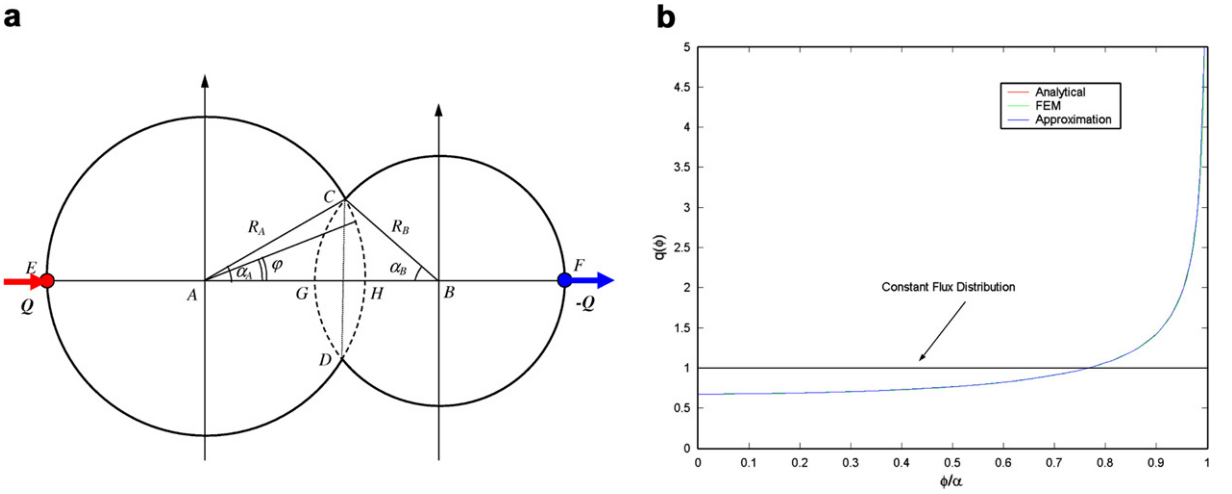

Fig. 7. (a) A two-disk contact system; (b) comparison of flux distribution on arc CHD.

This solution reveals that there are two singular points at $\phi = \pm\alpha_A$ where the flux is infinite.

For a special case where $R_A = R_B = R$, $\alpha_A = \alpha_B = \alpha = \pi/18$ $(= 10^\circ)$ and Q is chosen to be $2\alpha_A R$ so that $q(\phi) = -w(\phi)$, the distribution of the flux along the arc CHD, computed based on formula (39), is depicted in Fig. 7b. Due to symmetry, only one half is displayed. To assess the correctness of the analytical solution, the FEM result obtained by using a very fine mesh is also shown in the figure. An excellent agreement between the analytical and FEM solutions is clearly observed. A constant flux of 1, corresponding to the assumption made in the earlier development, is also drawn for comparison.

Fig. 7b shows that the actual flux is fairly constant in the central region but gradually increases towards the end of the arc (the intersection point of the two disks), at which the flux becomes infinite. A small discrepancy at the central region and a large difference towards the end between the constant flux assumption and the actual distribution are evident. In other words, formula (32) overestimates h_{ii} and thus introduces solution errors. Note however that any assumption made on the flux distribution will have little effect on the off-diagonal coefficients h_{ij}, as long as the two contact zones concerned are not too close.

Although singularity is present in the actual flux distribution, the temperature distribution in the contact zone is very close to a constant. In fact, the analytical solution indicates that for two disks of the same size, the temperature along the chord CD (refer to Fig. 7a) must be constant.

Based on the above analysis and observations, two solutions can improve the modelling accuracy of the discrete thermal element method. In the first approach, the analytical flux distribution function (38) is directly used in (17), which leads to the following new formula for h_{ii}

$$h_{ii} = -\frac{1}{\pi\kappa\alpha_i^2}\int_{-\alpha_i}^{\alpha_i}\int_{-\alpha_i}^{\alpha_i} w(\phi)\ln\left|\sin\frac{\theta-\phi}{2}\right|\mathrm{d}\phi\,\mathrm{d}\theta \tag{40}$$

where $w(\phi)$, defined in (39), can be viewed as a weighting function. This new formula should provide an improved value for h_{ii} in principle. However, there are some computational implications for its use in practice. Firstly, it is complex to evaluate $w(\phi)$. This issue is partially resolved for small contact angles by using a simpler approximate function to replace $w(\phi)$:

$$\bar{w}(\phi) = \frac{8\beta\alpha_A^2}{\pi[(\alpha_A+\phi)^{2\beta} + (\alpha_A-\phi)^{2\beta}]\left(\alpha_A^2-\phi^2\right)^{1-\beta}} \tag{41}$$

The excellent accuracy of this approximation is demonstrated in Fig. 7b for the special conditions given earlier. Secondly, due to the presence of the additional singularity in the integral (40), extra effort has to be made to numerically evaluate the integral. Although robust numerical procedures can be derived to deal with the singularities involved in the integration, a highly effective formula similar to (34) may no longer be available.

For the above reasons, the second approach for improving the accuracy of the discrete thermal element modelling is adopted. It is proposed that instead of introducing the weighting function in the computation of h_{ii}, a correction factor λ is directly applied to reduce the value of h_{ii} instead:

$$\hat{h}_{ii} = \lambda(\alpha_i) h_{ii} \tag{42}$$

The correction factor λ is determined by directly comparing the values evaluated by the two formulae (34) and (40) for the special conditions given in the above, with the latter being considered as the exact value. Table 1 lists the values of the correction factor for a set of contact angles. The corresponding value for an arbitrary contact angle can be obtained by a simple interpolation of the values given in the Table. Note that generally 2–3% of error is present under the special conditions in the original DTEM.

This approach retains the simplicity and effectiveness of the original method, and the resulting formula is referred to as the enhanced DTEM. Note that the correction values are established under the special heating conditions, therefore the approximation error of the DTEM cannot be completely eliminated in general situations. The performance of this enhanced version will be assessed through numerical validations to be presented in the next section.

4.2. Thermal contact resistance

In the above development, a perfect thermal contact condition is assumed between two contact surfaces. However, due to the surface roughness as well as other complex factors, a certain degree of thermal resistance is always present. Such a phenomenon can be readily accommodated in the current discrete thermal element framework. Basically thermal contact resistance can be simply modelled as a thermal 'bar' or 'spring'. When a thermal resistance of R_{TC} is taken into account at the contact zones of two particles, an equivalent thermal bar element is introduced as

$$\begin{bmatrix} Q_i^{(1)} \\ Q_i^{(2)} \end{bmatrix} = \frac{1}{R_{\mathrm{TC}}} \begin{bmatrix} 1 & -1 \\ -1 & 1 \end{bmatrix} \begin{bmatrix} T_i^{(1)} \\ T_i^{(2)} \end{bmatrix} \tag{43}$$

in which $T_i^{(1)}$ and $T_i^{(2)}$ are, respectively, the temperatures at the contact zones of the two particles; $Q_i^{(1)}$ and $Q_i^{(2)}$ are the corresponding heat fluxes.

This thermal contact element can be assembled as an individual element into the global conductivity matrix in the normal way. The only difference is that $T_i^{(1)}$ and $T_i^{(2)}$ are now two different variables, and thus the total order of the resulting global thermal conduction equations will be doubled if thermal resistance is considered at every contact zone.

5. Numerical validation and illustration

Two examples are provided below to further assess the solution error of the proposed method and to illustrate its effectiveness.

5.1. Finite element validation

The solution accuracy of the proposed discrete thermal element method with the two versions is first assessed against the finite element method. An assembly of 12 particles confined within an unit square with two vertical walls having prescribed temperatures, as shown in Fig. 8a, is used as an example. The conductivity κ is set to be 1. The dimensionless coordinates of the centres and radii of all the particles are listed in Table 2.

Table 1
Values of the correction factor λ for different contact angles α

α (°)	1	2.5	5	7.5	10	12.5	15	17.5	20
λ	0.9799	0.9762	0.9729	0.9707	0.9693	0.9682	0.9675	0.9672	0.9671

For geometrical overlap, there are in total 17 contact links/zones between the particles, plus 4 additional contact links with the walls. The numberings of the particles and the contact links are also given in the figure. The thermal conduction between the particles and the walls can be treated similarly to a particle/particle case. The left and right walls have a prescribed temperature of $T_1 = 1^\circ$ and $T_2 = 0^\circ$, respectively. All the contact angles, α, are within a narrow range of 5.2–6.2°. The values of n vary between 2 and 4; and the total number of the global system of equations is 17 after imposing the boundary conditions.

The corresponding finite element model using triangular elements is set up with all the contact zones being represented accurately. Several different mesh sizes, ranging from 0.02 to 0.0025, are used to provide a wider assessment to the proposed DTEM. Fig. 8b shows the coarsest mesh (mesh size = 0.02) with 3839 nodes and 2141 elements. For this mesh, each contact zone is discretized by one element. The results obtained from the finest mesh (mesh size = 0.0025), consisting of 122,579 nodes and 241,538 elements, are adopted as the exact values. Note that no effort has been made to use mesh adaptivity to optimize the finite element meshes. Thus, the sizes of the FE meshes used in terms of elements and nodes are indicative only.

The first comparison made between the FE models and the two discrete thermal element versions, standard and enhanced, is for the computed effective thermal conductivity, $\hat{\kappa}$, of the assembly, which is defined as

$$\hat{\kappa} = Q/(T_1 - T_0) = Q \tag{44}$$

where Q is the total heat flux flowing into the assembly.

For the enhanced DTEM version, a correction factor is applied to each diagonal term h_{ii}. The factor for the corresponding contact angle is obtained by linearly interpolating the values presented in Table 1.

Table 3 summarizes the computed effective conductivity for the different models together with the errors relative to the FE model of mesh size = 0.0025. It can be seen that the standard DTEM achieves a relative error of 5.16%, which is slightly larger than that of the finite element model with mesh density of 0.01 but smaller than that of 0.02. This is already an acceptable level for most engineering problems. It is also shown that the enhanced DTEM further reduces the error by more than half to 2.37% that is close to the accuracy achieved by the FE model with mesh size = 0.005. These results are thus very encouraging, particularly when taking into consideration the simplicity and the very small scale of the DTEM model. The remaining error is mainly due to the inaccurate description of the contact geometry which will be investigated later.

The average temperatures at the 17 contact zones are then compared. Table 4 lists the results from both versions of DTEM and FEM, where the FEM values are taken from the finest mesh, and DTEM-S and

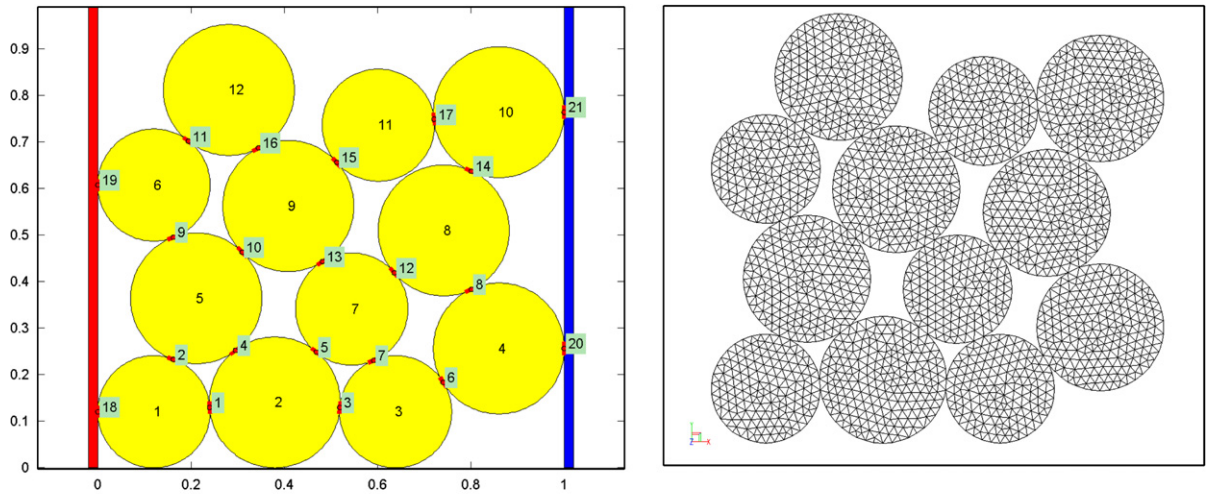

(a) Particle and contact link/zone numberings

(b) Mesh size=0.02; elements=3839; nodes=2414

Fig. 8. Example 1 – 12 particle system: (a) discrete particle model; and (b) finite element mesh.

Table 2
Example 1 – coordinates of centres and radii of particles

Number	*X*-coordinate	*Y*-coordinate	Radius
1	0.120000	0.120000	0.1206
2	0.379230	0.140000	0.1407
3	0.638459	0.120000	0.1206
4	0.860000	0.256087	0.1407
5	0.210758	0.363645	0.1407
6	0.120000	0.607291	0.1206
7	0.544396	0.340799	0.1206
8	0.741856	0.509942	0.1407
9	0.408143	0.562238	0.1407
10	0.860000	0.763796	0.1407
11	0.601482	0.736077	0.1206
12	0.280799	0.811604	0.1407

Table 3
Example 1 – comparison of computed effective conductivity $\hat{\kappa}$

	Model					
	FEM				DTEM	
Mesh size/version	0.02	0.01	0.005	0.0025	Standard	Enhanced
Effective $\hat{\kappa}$	0.3062	0.2931	0.2860	0.2824	0.2678	0.2757
Error (%)	8.41	3.79	1.27	–	5.16	2.37

Table 4
Example 1 – comparison of average temperatures at contact zones

Zone number	1	2	3	4	5	6	7	8	9
FEM	0.7216	0.7678	0.4964	0.6679	0.5217	0.2923	0.4340	0.2228	0.7807
DTEM-S	0.7208	0.7674	0.4965	0.6668	0.5218	0.2917	0.4337	0.2223	0.7803
Error (%)	0.104	0.056	0.030	0.176	0.011	0.220	0.067	0.233	0.044
DTEM-E	0.7211	0.7674	0.4964	0.6672	0.5217	0.2918	0.4338	0.2226	0.7803
Error (%)	0.072	0.057	0.007	0.116	0.017	0.158	0.049	0.073	0.050
Zone number	10	11	12	13	14	15	16	17	Average
FEM	0.6426	0.7719	0.3604	0.5056	0.2128	0.4648	0.6353	0.2657	–
DTEM-S	0.6420	0.7719	0.3598	0.5054	0.2124	0.4643	0.6350	0.2649	–
Error (%)	0.088	0.001	0.152	0.037	0.173	0.126	0.050	0.307	0.110
DTEM-E	0.6424	0.7717	0.3600	0.5054	0.2127	0.4646	0.6352	0.2652	–
Error (%)	0.038	0.034	0.119	0.034	0.056	0.056	0.021	0.172	0.066

DETM-E denote, respectively, the standard and enhanced versions of the DTEM. It shows that both DETM-S and DTEM-E have achieved much higher solution accuracies (comparing with the effective thermal conductivity), with averages of 0.11% and 0.066%, respectively. Again the enhanced DTEM is about two times more accurate than the standard DTEM. The fact that much higher accuracy is obtained for the temperature distribution than the flux distribution further indicates that the current enhanced DTEM still underestimates the particle conductivity by a relative constant factor and thus there is room to reduce the modelling error of the DTEM further.

For illustrative purposes, Fig. 9 depicts the average temperature distribution of the particles simulated by the DTEM-E and the temperature contour plot by the FEM.

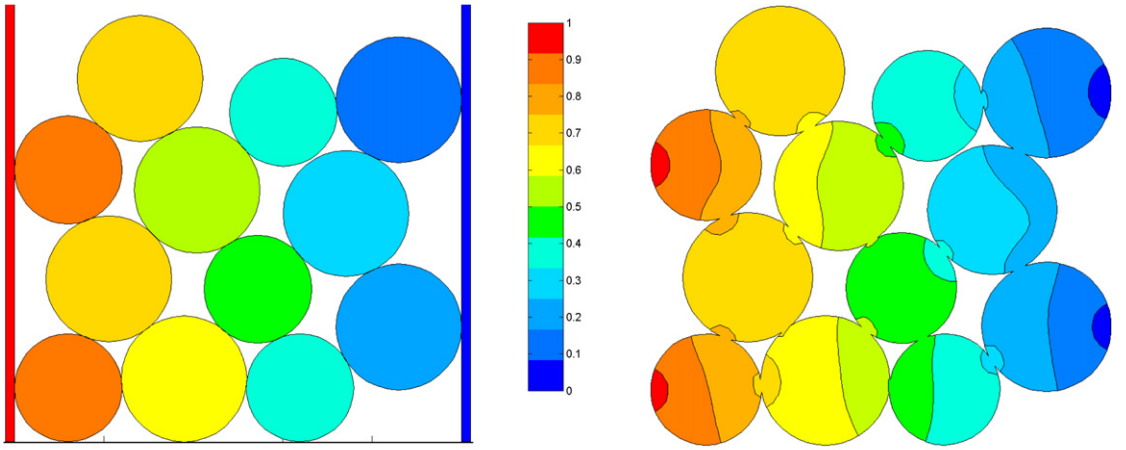

(a) Averaged particle temperature (b) Temperature contour

Fig. 9. Example 1 – Particle temperature distribution comparison: (a) DTEM; (b) FEM.

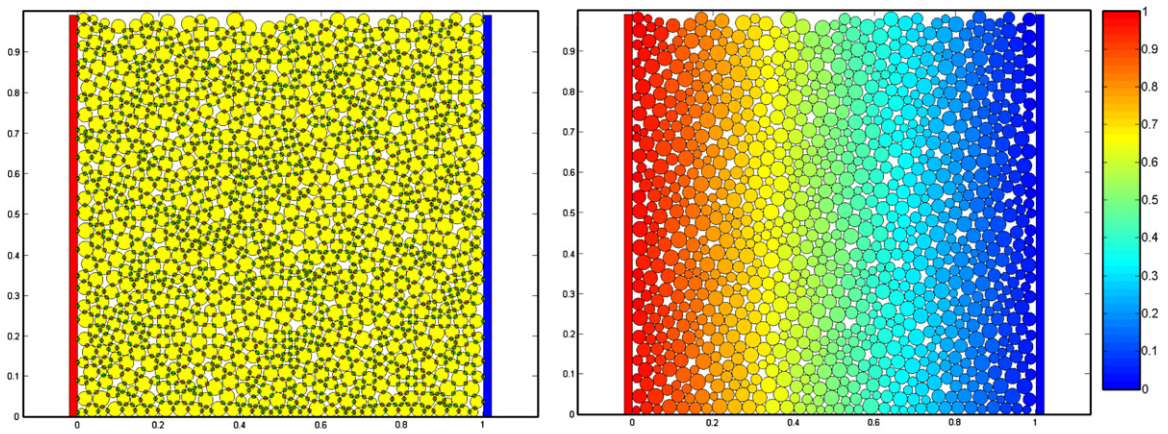

(a) Discrete thermal element model (b) Average particle temperature distribution

Fig. 10. Example 2 – 1084 particle system.

5.2. Illustrative example

The effectiveness of the DTEM is further demonstrated with this second example. The general problem setting is similar to the previous one except that the assembly consists of 1084 particles that are randomly generated by the advancing-front packing algorithm [24]. The sizes of particles are evenly distributed in the range $[0.01, 0.02]$. The average coordination number of the particles is 3.88 and there are 2102 contact links in total – which is the total number of unknown variables in the DTEM system. The corresponding discrete thermal element model is depicted in Fig. 10a, while the average particle temperature distribution simulated by the DTEM is illustrated in Fig. 10b, from which a realistic result is apparent. Note that much larger systems, with tens of thousands of particles, can also be easily simulated.

6. Concluding remarks

The present work has developed a novel discrete thermal element approach that not only provides a simple and accurate heat conduction model for particles but also can be employed to effectively simulate heat con-

duction in systems comprising a large number of particles. The method exhibits a number of attractive features.

Each particle is treated as an individual element with the number of (temperature) unknowns equal to the number of particles that it is in contact with. The element thermal conductivity matrix can be very effectively evaluated and is entirely dependent on the positions and contact angles of the associated contact zones/links, which are identified as the main characteristics of heat conduction in circular particles. The resulting global system of equations is determined by the topology of the particle contact links and its order equals the number of links.

Both the element and global conductivity matrices share the same form and properties (symmetry and sparsity, for instance) as its conventional thermal finite element counterpart. Each particle can thus be considered as a special finite element and, particularly, the whole solution procedure follows exactly the same steps as that involved in the finite element analysis. Another advantage is that the discrete thermal elements can be combined with finite elements and be readily incorporated into existing finite element programs.

There is no discretization error associated with the current approach. Apart from a slightly inaccurate geometry description for the contact zones for small contact angles, the most significant assumption made in the development of the discrete thermal element formulation is that the flux is constant over the contact zone. Based on the theoretical analysis, a simple enhanced version has been proposed to deal with the issue. The numerical assessment conducted indicates that the standard version performs exceptionally well for the temperature distribution, exhibiting about 5% of error for the flux for the given example, which is already within the acceptable level for engineering practice. The enhanced version further improves the accuracy.

Finally, the most important contribution of the present work is the development of a new numerical framework, within which more interesting and challenging thermal problems in particle systems can be more effectively tackled. For instance, 3D spherical particles can be treated in a similar manner; extension to transient problems is possible; a fully coupled mechanical–thermal analysis can be carried out; and further coupling with fluid flows becomes more tractable. These problems are currently being pursued and will be reported later.

Acknowledgments

This work is partially funded by the EPSRC of UK under Grant Nos. GR/R92318/01 and EP/C51520X/1. The support is gratefully acknowledged.

References

[1] H.C. Huang, A.S. Usmani, Finite Element Analysis for Heat Transfer, Springer-Verlag, London, 1994.
[2] C.A. Brebbia, J. Dominguez, Boundary Elements: An Introductory Course, McGraw-Hill Book Company, New York, 1989.
[3] M. Bonnet, Boundary Integral Equation Methods for Solids and Fluids, John Wiley & Sons Ltd., London, 1995.
[4] W.W.M. Siu, S.H.-K. Lee, Transient temperature computation of spheres in three-dimensional random packings, International Journal of Heat and Mass Transfer 47 (5) (2004) 887–898.
[5] G.J. Cheng, A.B. Yu, P. Zulli, Evaluation of effective thermal conductivity from the structure of a packed bed, Chemical Engineering Science 54 (1999) 4199–4209.
[6] Zhaosheng Yua, Xueming Shaob, Anthony Wachs, A fictitious domain method for particulate flows with heat transfer, Journal of Computational Physics 217 (2006) 424–452.
[7] J. Kuipers, K. van Duin, F. van Beckum, W. van Swaaij, A numerical model of gas-fluidized beds, Chemical Engineering Science 47 (1992) 1913–1924.
[8] Y. Tsuji, T. Kawaguchi, T. Tanaka, Discrete particle simulation of two-dimensional fluidized bed, Powder Technology 77 (1) (1993) 79–87.
[9] Y. Shimizu, Three-dimensional simulation using fixed coarse-grid thermal-fluid scheme and conduction heat transfer scheme in distinct element method, Powder Technology 165 (3) (2006) 140–152.
[10] S. Chen, G. Doolen, Lattice Boltzmann method for fluid flows, Annual Review of Fluid Mechanics 30 (1998) 329–364.
[11] P.A. Cundall, O.D.L. Strack, A discrete numerical model for granular assemblies, Geotechnique 29 (1) (1979) 47–65.
[12] B.K. Cook, D.R. Noble, J.R. Williams, A direct simulation method for particle–fluid systems, Engineering Computations 21 (2–4) (2004) 151–168.
[13] K. Han, Y.T. Feng, D.R.J. Owen, Coupled lattice Boltzmann and discrete element modelling for particle–fluid problems, Computers & Structures 85 (11–14) (2007) 1080–1088.

[14] K. Han, Y.T. Feng, D.R.J. Owen, Numerical simulations of irregular particle transport in turbulent flows using coupled LBM-DEM, Computer Modeling in Engineering & Science 18 (2) (2007) 87–100.
[15] Y.T. Feng, K. Han, D.R.J. Owen, Coupled lattice Boltzmann method and discrete element modelling of particle transport in turbulent fluid flows: computational issues, International Journal For Numerical Methods in Engineering 72 (9) (2007) 1111–1134.
[16] K. Han, Y.T. Feng, D.R.J. Owen, Modelling of thermal contact resistance within the framework of the thermal lattice Boltzmann method, International Journal of Thermal Sciences, in press. doi:10.1016/j.ijthermalsci.2007.11.007.
[17] X. He, S. Chen, G.D. Doolen, A novel thermal model for the lattice Boltzmann method in incompressible limit, Journal of Computational Physics 146 (1998) 282–300.
[18] H.S. Carslaw, J.C. Jaeger, Conduction of Heat in Solids, second ed., Oxford University Press, 1965.
[19] G.F. Carrier, C.E. Pearson, Partial Differential Equations: Theory and Technique, Academic Press, London, 1976.
[20] K.L. Johnson, Contact Mechanics, Cambridge University Press, 1985.
[21] A.H. Stroud, D. Secrest, Gaussian Quadrature Formulas, Prentice Hall, 1966.
[22] Y.T. Feng, D.R.J. Owen, An augmented spatial digital tree algorithm for contact detection in computational mechanics, International Journal For Numerical Methods in Engineering 55 (2002) 556–574.
[23] Y.T. Feng, On the discrete dynamic nature of the conjugate gradient method, Journal of Computational Physics 211 (1) (2006) 91–98.
[24] Y.T. Feng, K. Han, D.R.J. Owen, Filling domains with disks: an advancing front approach, International Journal For Numerical Methods in Engineering 56 (2003) 699–713.